Annual Journal of Hydraulic Engineering, JSCE, Vol.50, 2006, February

NONLINEAR ANALYSIS OF SPATIAL VARIATION OF VELOCITY PROFILE IN A PRESSURIZED LAMINAR FLOW BETWEEN WAVY BOUNDARIES

Prosper MGAYA[1], Takashi HOSODA[2] and Kiyoshi KISHIDA[3]

[1] Graduate student, Dept. of Urban Management Kyoto University
[2] Member of JSCE, Professor, Dept. of Urban Management Kyoto University
[3] Member of JSCE, Associate Professor, Dept. of Urban Management Kyoto University

A nonlinear analysis procedure has been proposed to simulate the spatial variation of velocity profile of pressurized laminar flows between wavy boundaries as an idealized flow model in rock fractures. The main objective of this analysis is to refine the depth averaged flow model for a rock joint, reflecting the results of this analysis. The analysis is based on an assumed general form of velocity profile in the direction of flow, whereby the unknowns are determined through the use of the continuity and momentum equations. Comparison is made between the 2D-vertical model's results and the nonlinear solution through which the applicability of the analysis is verified. The nonlinear solution shows good agreement with the 2D-vertical model's results especially for small amplitude-to-wavelength ratio of the wavy boundaries, but enough to reveal the velocity profile's deformation.

Key Words: *Nonlinear analysis, velocity profile, rock fracture, wavy boundaries*

1. INTRODUCTION

Pressurized laminar flow between wavy boundaries with sinusoidal variations has been taken as a simpler phenomenon which helps in understanding the behavior of complex flows such as in enhancement of heat and mass transfer and flow in fractures[1),2),3)]. However, the problem has always been that in order to easily describe the insight of flow behavior velocity distribution has to be known. The assumption has always been made for the velocity distribution to be parabolic in transverse direction. Based on this assumption a 2-D depth averaged flow model for predicting the flow in a rock joint was developed[3)].

In fact the velocity distribution is not always parabolic; depending on the hydraulic conditions and geometry of the boundaries in some cases flow separation may occur. Therefore the parabolic assumption may introduce significant computational errors[4)]. This problem can be overcome if the relation between the spatial velocity variation and the parameters describing physical boundaries and flow conditions is established.

As the genesis of establishing this relation, in this paper, the procedure and the results of nonlinear analysis of spatial velocity variation between the wavy boundaries are presented. The computational results of 2D-vertical model are also presented to verify the nonlinear analysis. The results of this analysis will be utilized in the next stage for refining the depth averaged flow model to include the effect of the local change of velocity distribution.

2. NONLINEAR ANALYSIS

The analysis is achieved through the use of Navier - Stokes equation and the assumed general form of equation for velocity profile variation along the spatial direction. We consider here Newtonian, incompressible flows with constant properties governed by the Navier-Stokes equations.

(1) Problem formulation

It is assumed that the flow occurs between two sinusoidal boundaries in the x-z plane refer **Fig.1**. The boundaries are defined by the distance z_s and z_b from the horizontal x- axis described by the following expressions.

$$z_s = \delta\cos(nx+\phi_s)+\Delta$$
$$z_b = \delta\cos(nx) \quad (1)$$
$$D = z_s - z_b$$

where δ is amplitude of variation of the wavy boundaries, Δ is the average distance between the wavy boundaries, ϕ_s is phase angle, D is the aperture and n is wave number $(=2\pi/\lambda)$. In this study ϕ_s is set to π.

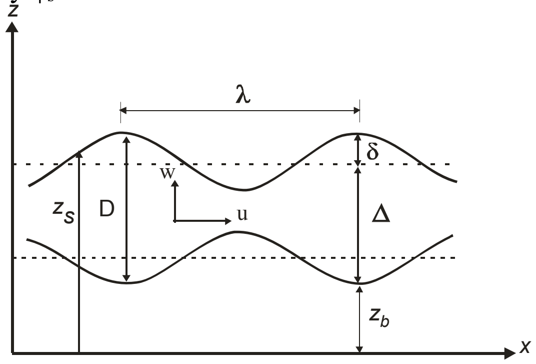

Fig.1 Illustration of an idealized flow setup

(2) Basic equations

In order to capture the variation of velocity profile along the spatial variation of the wavy boundaries, the analysis is based on steady state 2D-vertical Navier- Stokes and continuity equations (2)-(4).

Continuity equation

$$\frac{\partial u}{\partial x}+\frac{\partial w}{\partial z}=0 \quad (2)$$

Momentum equations

$$u\frac{\partial u}{\partial x}+w\frac{\partial u}{\partial z}=-\frac{1}{\rho}\frac{\partial p}{\partial x}+\nu\left(\frac{\partial^2 u}{\partial x^2}+\frac{\partial^2 u}{\partial z^2}\right)+g_x \quad (3)$$

$$u\frac{\partial w}{\partial x}+w\frac{\partial w}{\partial z}=-\frac{1}{\rho}\frac{\partial p}{\partial z}+\nu\left(\frac{\partial^2 w}{\partial x^2}+\frac{\partial^2 w}{\partial z^2}\right)+g_z \quad (4)$$

where u and w are velocities in x and z directions respectively, p is pressure, ν kinematic viscosity, ρ is fluid density (kg/m^3) and g is the gravitational acceleration (m/s^2).

(3) Procedure of nonlinear analysis

In this analysis a velocity distribution is firstly assumed with parameters which have to be determined. The velocity distribution herein considered/assumed is defined by the following expression.

$$u = u_0 + u' \quad (5)$$

where $u_0 = a_0(\eta-\eta^2)$, $\eta = \dfrac{z-z_b}{D}$ and

$$u' = a_1(\eta-\eta^2)+a_2(\eta^4-2\eta^2+\frac{3}{2}\eta^2-\frac{1}{2}\eta)$$

u_0 is the velocity component with parabolic shape equivalent to velocity profile of the 2D depth averaged flow model and u′ is the velocity component which includes the effect of velocity

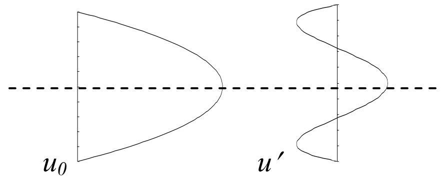

Fig.2 An idealized velocity distribution

profile distortion. This means when u' is neglected the total velocity distribution (u) resembles that of depth averaged flow model (i.e. parabolic velocity distribution). Note that both components are symmetric about the line of symmetry refer **Fig.2**.

The parameters a_0, a_1 and a_2 are assumed to vary in the spatial direction such that:

$$a_0, a_1, a_2 = f(\delta/\lambda, \delta/\Delta \text{ and } S) \quad (6)$$

where S = hydraulic gradient in the direction of flow.

Since we consider flow between wavy boundaries with sinusoidal perturbation, we further assume that the parameters a_0, a_1 and a_2 can be expressed by periodic functions[6)]. Based on this fact, parameters a_1 and a_2 are assumed to vary in the spatial direction according to the following expressions.

$$a_1 = \delta_{a1}\cos(nx+\theta_{a1}) = a_{1c}\cos(nx) - a_{1s}\sin(nx) \quad (7)$$

$$a_2 = \delta_{a2}\cos(nx+\theta_{a2}) = a_{2c}\cos(nx) - a_{2s}\sin(nx) \quad (8)$$

where $a_{1c}=\delta_{a1}\cos(\theta_{a1})$, $a_{1s}=\delta_{a1}\sin(\theta_{a1})$, similarly for a_2; δ_{ai} is the amplitude of variation and θ_{ai} is phase angle.

Using the expression for discharge per unit width $q = UD$, the relation for parameter a_0 is derived as following.

$$\int_{\eta=0}^{\eta=1} u\,d\eta = \frac{1}{6}a_0 = U \qquad \Rightarrow a_0 = \frac{6q}{D} \quad (9)$$

where U is the bulk velocity.

Based on the assumed velocity distribution and momentum equations it is evident that the following unknowns are to be solved. The velocity w, pressure p, discharge q and parameters a_{1c}, a_{1s}, a_{2c} and a_{2s}

If the expression for the velocity component u' is integrated with respect to z-direction it vanishes (equal to zero); we use this fact to derive the relations for the parameters a_{2s} and a_{2c}.

$$a_{2s} = \frac{10}{6}a_{1s} \text{ and } a_{2c} = \frac{10}{6}a_{1c} \quad (10)$$

Then the expression for the velocity `$w$` is derived using the assumed velocity distribution and the continuity equation as follows.

$$w = -\int_{z_b}^{z} \frac{\partial u}{\partial x} dz = -D \int_{\eta=0}^{\eta} \frac{\partial u}{\partial x} d\eta$$

$$w = -D\left(A_0 \eta + \frac{1}{2} A_1 \eta^2 + ... + \frac{1}{5} A_4 \eta^5 \right) \quad (11)$$

$A_i = f\,(q,\ a_{1s},\ a_{1c}, \delta,\ \lambda,\ \Delta \text{ and } S)$

The formula for pressure distribution across the aperture *'D'* is derived by integrating the equation of motion in z-direction.

$$p = p_D + \int_z^{z_s} \left[w \frac{\partial w}{\partial z} + u \frac{\partial w}{\partial x} + g + \nu \frac{\partial^2 w}{\partial z^2} \right] \quad (12)$$

where p_D is the pressure at the top wavy wall/boundary. Note that the term $\nu\, \partial^2 w / \partial x^2$ is assumed to be negligible.

Based on the previous study on flows in wavy boundaries it is evident that the pressure variation in the spatial direction can also be defined by a periodic function[5]. Therefore, in this study we assume the pressure p_D to be composed of two components.

$$p_D = p_0 + p' \quad (13)$$

p_0 is the pressure component for undisturbed flow (for parallel plate flow) and p'= wave induced pressure component. We further express the pressure p' with the following general periodic function;

$$\frac{p'}{\rho g} = \delta_p \cos\left(nx + \phi_p\right) \quad (14)$$

Then, the expressions for *w, p, u* are substituted to Eqs.(3) and its integral form. After some manipulation and equating the coefficients of η^0 we obtain two equations with sine and cosines. We further equate coefficient of equal sine and cosines through which the following set of equations is obtained with unknown variables q, a_{1s}, a_{1c}, p_{1c} and p_{1s}.

$$\left.\begin{aligned}
&D_{11} q + D_{12} p_s + D_{13} a_{1c} + D_{10} = C_1 \\
&D_{22} p_c + D_{23} a_{1s} + D_{20} = C_2 \\
&D_{31} q + D_{32} p_s + D_{33} a_{1c} + D_{30} = C_3 \\
&D_{41} q + D_{42} p_s + D_{43} a_{1c} + D_{40} = C_4 \\
&D_{52} p_c + D_{53} a_{1s} + D_{50} = C_5
\end{aligned}\right\} \quad (15)$$

where D_{nm} are known coefficients such that $D_{nm}=f(S,\Delta,\lambda,\delta,g)$, and C_n are the nonlinear parts $C=f(S,\Delta,\lambda,\delta,g,\ q,\ a_{1s},\ a_{1c},\ p_{1c} \text{ and } p_{1s})$. Only the following coefficient D_{10}, D_{11}, D_{12}, D_{13} and part of C_1 are given in this paper.

$$D_{10} = gS(6\delta^2 \Delta + \Delta^3)$$

$$D_{11} = \nu(-18(n\delta)^2 - 12)$$

$$D_{12} = -3(\delta^3 + 3\Delta^2 \delta)$$

$$D_{13} = \nu\left(\frac{4}{3}\delta\right)$$

$$C_1 = \left(\frac{4}{105} n\delta\Delta\right) q a_{1s} - \left(\frac{12}{2835} n\delta^2 \Delta\right) a_{1c} a_{1s} + ...$$

The set of Eqs.(15) are solved simultaneously through the iteration method. Firstly, it is assumed that the nonlinear part of each equation is zero, and then the linear parts of equations are solved for the initial solution which allows to initiate the iteration procedure. Then the calculated variables are used to obtain the value of nonlinear parts for the next iteration. This procedure is repeated until the criterion is satisfied that the difference of solution between consecutive iterations is zero. Then the values obtained are regarded as the solution of the equations.

3. MODEL VERIFICATION

The nonlinear analysis solution herein derived is verified through a simplified numerical solution of a 2D-vertical model in a generalized coordinate system. This is based on the fact that 2D- vertical model captures the characteristics of vertical variation of velocity profile. The governing equations consist of continuity and momentum equations (16) – (18).

(1) Basic equation

Continuity equation

$$\frac{\partial U}{\partial \xi} + \frac{\partial W}{\partial \eta} = 0 \quad (16)$$

Momentum equations

ξ - direction

$$\frac{\partial u}{\partial t} + \frac{1}{J}\left(\frac{\partial}{\partial \xi} Uu + \frac{\partial}{\partial \eta} Wu \right) = \frac{1}{J} \nu \nabla^2_{\xi,\eta} u - \left(\xi_x \frac{\partial \varphi}{\partial \xi} + \eta_x \frac{\partial \varphi}{\partial \eta} \right) + g_\xi \quad (17)$$

η - direction

$$\frac{\partial w}{\partial t} + \frac{1}{J}\left(\frac{\partial}{\partial \xi} Uw + \frac{\partial}{\partial \eta} Ww \right) = \frac{1}{J} \nu \nabla^2_{\xi,\eta} w - \left(\xi_y \frac{\partial \varphi}{\partial \xi} + \eta_y \frac{\partial \varphi}{\partial \eta} \right) + g_\eta \quad (18)$$

where

$$\nabla^2_{\xi,\eta} u = \frac{\partial}{\partial \xi}\left(\alpha_1 \frac{\partial u}{\partial \xi} + \alpha_2 \frac{\partial u}{\partial \eta} \right) + \frac{\partial}{\partial \eta}\left(\alpha_2 \frac{\partial u}{\partial \xi} + \alpha_3 \frac{\partial u}{\partial \eta} \right)$$

similarly for $\nabla^2_{\xi,\eta} w$; $\alpha_1 = J\left(\xi_x^2 + \xi_y^2\right)$; $\varphi = p/\rho$

$\alpha_2 = J\left(\xi_x \eta_x + \eta_y \xi_y \right)$; $\alpha_1 = J\left(\eta_x^2 + \eta_y^2\right)$, U and W are contravariant velocities in ξ and η directions respectively, J is Jacobian of transformation and g_ξ and g_η are gravitational components in generalized coordinate system in m/s^2. Other quantities take the same definition as defined previously.

(2) Numerical procedure

The numerical solution is obtained through the use of Fractional-Step method using the finite difference scheme[7]. The variables are arranged in a staggered grid system refer **Fig.3.** Note that uniform grid in η-direction was used and therefore in order to capture the velocity variations in troughs, very fine grids are used.

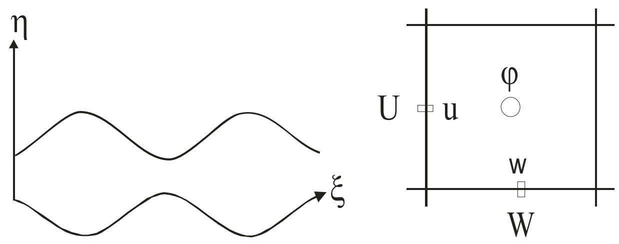

Fig.3 Illustration of coordinate system and arrangement of flow variables

The Fractional-Step method consists of three steps. In the first step, a provisional value of the velocity u^* is computed from Eq.(19) which is the momentum equation without the pressure gradient term; similarly for the velocity `$w$` in z-direction. The convective terms are discretized using the QUICK scheme while the central different scheme is used for the diffusion terms.

$$\frac{u^* - u}{\Delta t} = -\frac{1}{J}\left(\frac{\partial}{\partial \xi}Uu + \frac{\partial}{\partial \eta}Wu - \nu\nabla^2_{\xi,\eta}u\right) + g_\xi \quad (19)$$

Secondly, the pressure field is obtained through solving the Poisson equation Eq.(20) using the iteration technique. The Poisson equation is derived by taking the divergence of Eqs. (17) and (18) without the convection and diffusion terms, with the condition that u^{n+1} must be divergence free vector.

$$\nabla^2 \varphi^{n+1} = \frac{1}{\Delta t}\nabla U \quad (20)$$

Then the velocity at the next time step ($n+1$) is obtained through updating the auxiliary velocity u^* using equation (21).

$$\frac{u^{n+1} - u^*}{\Delta t} = \left(\xi_y \frac{\partial \varphi}{\partial \xi} + \eta_y \frac{\partial \varphi}{\partial \eta}\right) \quad (21)$$

During numerical simulation, we adopted the no flow boundaries at the walls (Γ), and for pressure we used the boundary condition $\partial\varphi/\partial\mathbf{n}=0$ on Γ. This condition is derived from the Neumann condition using the assumption that u^* converges to the value of u^{n+1} and that converges to exact solution when small time step is used[7].

4. RESULTS AND DISCUSSION

Results of nonlinear analysis are presented and compared with the solution of 2D-vertical model. Here, we investigate the variation of velocity profile based on different flow conditions and geometry of the wavy profile. The geometry of the profile is characterized using the amplitude-to-wavelength ratio δ/λ while the average aperture is kept constant (Δ=2mm). On the other hand we characterize the hydraulic condition through the hydraulic gradient S.

For the results herein presented we consider relatively small ratio δ/λ of order less that 0.1. This is because we could not get solution for relatively high amplitude-wavelength ratio beyond 0.1. However this ratio is still sufficient to describe the spatial velocity variation.

All variables are nondimensionalized; the velocity is nondimensionalized using the bulk velocity U_0 for an equivalent flow in parallel plate model with distance apart equal to average aperture Δ. The spatial distance (x) by wavelength (λ) of variation and the discharge (q) by the discharge (q_0) for equivalent discharge that could flow in parallel plate model for the same hydraulic gradient S.

We first compare the results through ability of the models to simulate flows resistance. **Fig.4** shows the resistance to flow characterized by the variation of discharge with regard to δ/λ . The ratio δ/λ has always been used as the measure of wall roughness; the higher the ratio δ/λ the higher wall roughness. Good agreement is observed and that the flow resistance increases with increase of wall roughness. This trend has also been reported in the previous studies e.g. Brown et al. [1] and Zimmerman et al.[2].

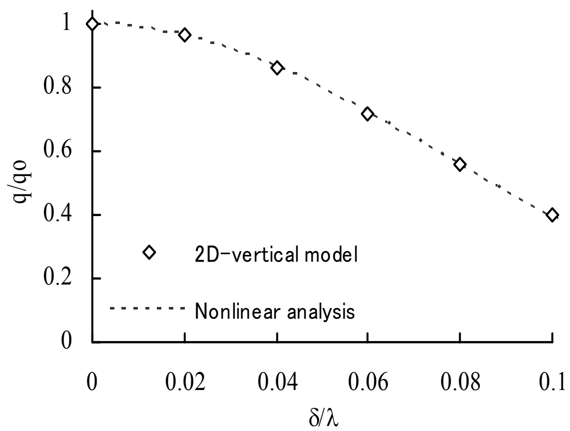

Fig.4 Flow resistance characterized by the ratio δ/λ for hydraulic gradient S = 0.005

Fig.5 presents the velocity field through the middle oscillation of roughness δ/λ= 0.04 and hydraulic gradient S=0.02. **Figs.5a** and **5b** display a vector distribution for nonlinear and 2D-vertical numerical solution. Both figures display some important features that at constrictions (point P1) the vector distribution is qualitatively parabolic and parallel to x-axis. The direction of the vectors spread or fans out as the aperture of the profile increases to P2 so as the vector next to the walls becomes parallel to the wall and vectors along the centerline remain parallel to the x-axis. However it is important to note that for the nonlinear analysis, the velocity vector does not fan enough to be parallel to walls as the aperture increases (i.e. the vectors are parallel to the horizontal axis). **Figs.5c** and **5d** displays vertical distribution of velocity u_x for nonlinear analysis, 2D-vertical model and the parabolic distribution assumed in the previous studies given by Eq. (22)[1),2),3),4)]

$$u = \varepsilon_0(\eta - \eta^2) \Rightarrow \varepsilon_0 = \frac{6q}{D} \tag{22}$$

It is observed that at constrictions all results are close to the ideal solution, while as the aperture increases the solutions for 2D-vertical model and nonlinear analysis deviates from the ideal solution. However, no flow separation can be observed. Generally good agreement between the 2D-vertical model and nonlinear analysis exists.

Fig.6 presents the similar velocity field but with increased roughness ratio to δ/λ= 0.08. Nearly the same characteristics as for **Fig.5** are observed. But it is important to note that at constrictions the velocity distribution is still close to the ideal solution.

However, as the aperture increases the velocity profiles significantly deviates from the ideal solution. Also it is interesting to note that both 2D-vertical numerical and nonlinear analysis results have shown flow separation at point P2.

We further investigate the effect of variation of hydraulic condition through changing the hydraulic gradient from S=0.005 to S= 0.02. **Fig.7** shows the variation of flow resistance with regard to hydraulic gradient variation. It can be observed that the increase of hydraulic gradient results into increase of flow resistance.

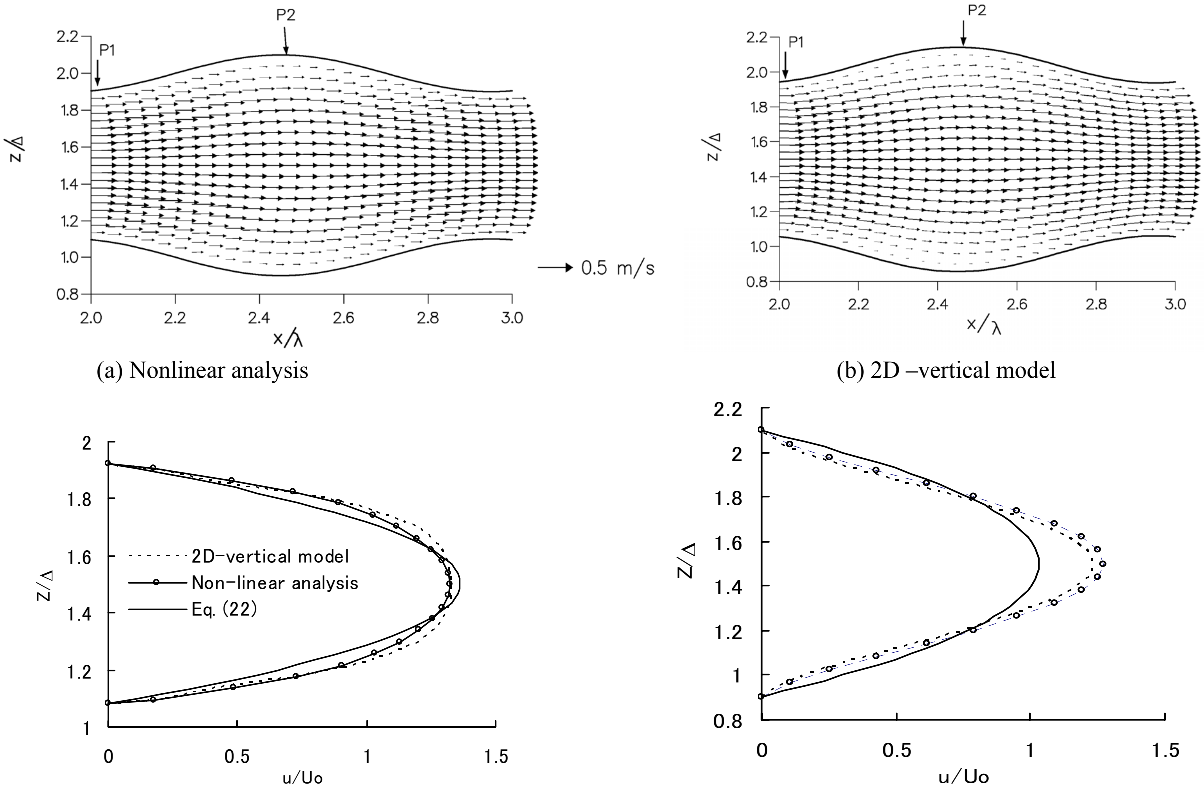

(a) Nonlinear analysis

(b) 2D –vertical model

(c) Velocity distribution at P1 (x/λ =2)

(d) Velocity distribution at P2 (x/λ = 2.5)

Fig.5 Nonlinear and 2D-vertical model numerical results. (a & b) Flow vector distribution and (c & d) velocity profile for δ/λ=0.04 and hydraulic gradient S = 0.02

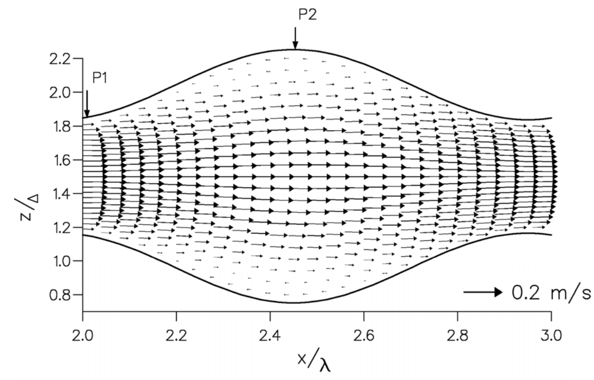

(a) Nonlinear analysis solution

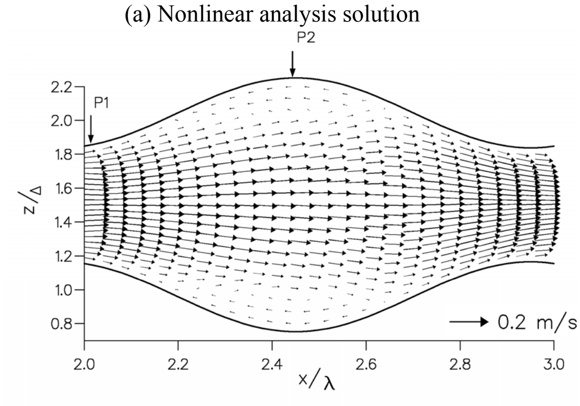

(b) 2D –vertical model

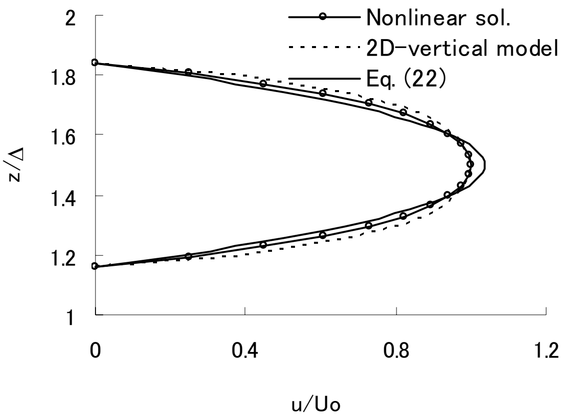

(c) Velocity distribution at P1 (x/λ =2)

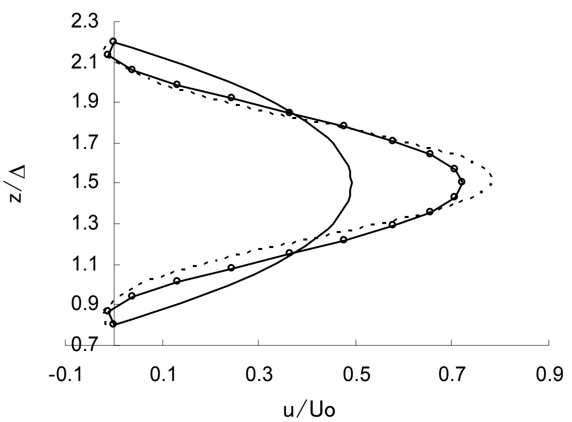

(d) Velocity distribution at P2 (x/λ = 2.5)

Fig.6 Nonlinear and 2D-vertical model results. (a & b) Flow vector distribution and (c & d) velocity profile for δ/λ=0.08 and hydraulic gradient S = 0.02

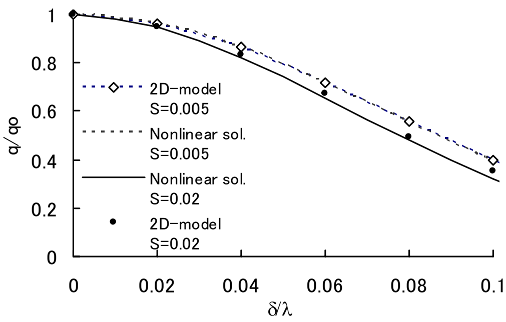

Fig.7 Flow resistance characterized by the ratio δ/λ for hydraulic gradient S = 0.005 and S=0.02

5. CONCLUSION

The proposed nonlinear analysis of velocity distribution has shown its ability to simulate the spatial velocity profile variation. The analysis can be used as long as the amplitude-to-wavelength ratio $\delta/\lambda \leq 0.1$. The simulations clearly demonstrate that the velocity profile between boundaries with wavy patterns can significantly deviate from the parabolic profile. Further analysis is underway using a more general sinusoidal fracture topography; through which a relation between the fracture's geometry and hydraulic conditions will be developed and then used in refining the 2D depth averaged flow model. This will be reported in the following paper.

REFERENCES

1) Brown, S. R., Stockman, H.W., and Reeves S.J: Applicability of Reynolds equation for modeling fluid flow between rough surfaces, *Geophysical Res. Lett.,* 22(18), pp.2537-2540, 1995.
2) Zimmerman, R.W., Kumar, S., Bodvarsson, G.S.: Lubrication theory analysis of the permeability of rough-walled fractures, *Int. J. Rock Mech. Min. Sci. & Geomech. Abstr.,* Vol. 28,No.4, pp.325-331, 1991.
3) Mgaya P.L., Kishida K., and Hosoda T: Estimation of flow behavior on rock joints using the depth averaged flow model, *J. of Applied Mechanics,* Vol.7, pp.1013-1021, 2004.
4) Brush B.J. and Thomson N.R.: Fluid flow in synthetic rough-walled fractures: Navier-Stokes, Stokes and local cubic law simulations, *Water Resources Res.,* Vol. 39, No.4, pp. SBH5-1, 2003.
5) Zilker D.P. and Hanratty: Influence of amplitude of a solid wavy wall on a turbulent flow, *J. Fluid Mechanics,* Vol. 82, pp. 29-51, 1977.
6) Floryan J.M.: Centrifugal instability of couette flow over a wavy wall, *Physics of fluids,* Vol. 14 No.1, pp. 312-322, 2002.
7) Peyret R. and Taylor T.D.: Computational methods for fluid flow, Springer-Verlag, New York, 1983.

(Received September 30, 2005)